Time-Resolved Measurements of OH during Auto-ignition of Syngas with Trimethylsilanol and Hexamethyldisiloxane

John H. Kim[a,], Andrew B. Mansfield[b], Miles A. Burnett[a], Robert S. Tranter[c], Margaret S. Wooldridge[a,d],*

[a]Department of Mechanical Engineering, University of Michigan, Ann Arbor, MI, US

[b]School of Engineering, Eastern Michigan University, Ypsilanti, MI, US

[c]Chemical Sciences and Engineering Division, Argonne National Laboratory, Lemont, IL, US

[d]Department of Aerospace Engineering, University of Michigan, Ann Arbor, MI, US

Abstract (100-300 words)

The effects of trimethylsilanol (TMSO) and hexamethyldisiloxane (HMDSO) addition on OH time histories during syngas (H_2 and CO) ignition were investigated using the University of Michigan rapid compression facility. Experiments spanned temperatures of 1010 – 1080 K, at a pressure of approximately 5 atm. Syngas mixtures of 1.2% H_2/2.8% CO/20% O_2 by volume (balance N_2 and Ar) provided a baseline for comparison with mixtures that included 100, 200, and 1000 ppm of the TMSO and 100 ppm of HMDSO. Narrow-line ultraviolet laser-absorption was used to measure OH mole-fraction during ignition. The addition of TMSO and HMDSO significantly shifted the OH time-histories earlier in time, by up to 51%, compared with the baseline syngas mixture. The

value of the maximum OH mole fraction was consistent between the 100 and 200 ppm TMSO mixtures and the 100 ppm HMDSO mixtures, but the maximum OH increased significantly with the 1000 ppm TMSO mixtures. The OH data indicate TMSO and HMDSO were not direct sources of OH radicals. Analysis further indicates the TMSO and HMDSO decompose rapidly followed by reactions that enhance the production of H atoms, and the increased reactivity observed is via the $H + O_2 = OH + O$ reaction.

Keywords: Trimethylsilanol, hexamethyldisiloxane, ignition; OH

---

*Corresponding author.

Novelty and Significance Statement

This study represents a significant improvement in understanding the combustion chemistry of siloxanes. It provides the first quantitative measurements of OH concentration during syngas ignition with trimethylsilanol (TMSO) and hexamethyldisiloxane (HMDSO). The experiments offer critical data for validating and improving siloxane reaction mechanisms. The integration of experimental data and modeling approach emphasizes the challenges in accurately representing silicon-based compounds in combustion systems. This work enhances capabilities of kinetic modeling and expands the knowledge of organosilicon compound behavior under high-temperature and high-pressure conditions.

Authors Contributions statement

J. H. K.: Investigation, Data curation, Visualization, Writing – original draft.

A. B. M.: Conceptualization, Investigation, Writing – review & editing.

M. A. B.: Investigation, Data curation, Writing – review & editing.

M. S. W.: Conceptualization, Investigation, Supervision, Writing – review & editing.

R. S. T.: Supervision, Writing – review & editing

1. Introduction

Syngas, a fuel mixture primarily composed of hydrogen (H_2) and carbon monoxide (CO), plays a significant role in contemporary energy and chemical manufacturing systems. Syngas can be produced from a range of renewable and non-renewable sources, including coal, natural gas, biomass, municipal waste, and also through 'solar-to-fuel' processes. Some syngas production pathways, particularly biomass waste-to-energy processes, can reduce carbon emissions and potentially enable carbon negative pathways for power and chemical manufacturing systems [1,2]. Utilization of biomass-derived syngas in combustion systems can present practical challenges related to the existence of trace species, including compounds that contain silicon, nitrogen, and sulfur [3,4,5]. Previous studies have investigated the effects of impurities on syngas combustion properties, providing valuable insights into ignition delay times and flame behaviors. Mathieu et al. [6,7,8] demonstrated that NH_3 generally had minimal impact on ignition delay times, while CH_4 significantly enhanced reactivity via $CH_4 + OH = CH_3 + H_2O$ reactions. On the other hand, H_2S showed dual behavior, where H_2S reduced ignition delay times under conditions dominated by HO_2 radicals, but increased ignition delay times when OH radicals were dominant. Additionally, H_2S exhibited an inhibiting effect on laminar flame speed but only for high concentrations [8]. These studies provided critical insights on how nitrogen and sulfur-based impurities affect syngas combustion under various conditions. Our work extends understanding on silicon-containing species, which are critical, yet less studied components of waste-derived syngas.

Although often at low concentrations (part-per-million (ppm) scale), these trace components have been shown to significantly affect the combustion properties of syngas including changes in reactivity, heat release rates, thermal efficiencies, flame stabilities, emissions, and other important performance characteristics [3,4, 9 , 10 , 11]. In addition to significant impact on

combustion behavior, Si-based siloxane compounds are well known to cause deposits leading to major fouling and hardware damage in combustion systems [10,12,13]. Understanding the effects of trace siloxanes on syngas combustion behavior and the processes controlling formation of solid deposits are critical to the successful utilization of these fuels. An added complication is the diversity of silicon-organic compounds relevant to waste-to-energy combustion systems, which include silanols like trimethylsilanol ($(CH_3)_3SiOH$, TMSO), linear siloxanes like hexamethyldisiloxane ($(CH_3)_3SiOSi(CH_3)_3$, HMDSO) and ring siloxanes like hexamethylcyclotrisiloxane ($C_6H_{18}O_3Si_3$) [10,133].

Fundamental studies of siloxane combustion kinetics are currently limited, and gas-phase siloxane reaction chemistry remains largely uncertain or unknown. Most prior work has focused on the particle formation processes with emphasis on silica nanoparticle synthesis (e.g., [14,15,16]) due to the importance of siloxanes in materials production. There has been less emphasis on the fuel consumption and thermal decomposition reactions that are important for heat and power applications. TMSO and HMDSO are the focus of the current work due to the importance of these compounds in waste water treatment and landfill biogas [13]. Previous ignition studies of mixtures of syngas and TMSO or HMDSO by Mansfield and Wooldridge [3] and later work by Schwind and Wooldridge [4] revealed the addition of these siloxanes at mole fraction levels from 100 to 1000 ppm significantly enhanced syngas reactivity; specifically resulting in shorter auto-ignition delay times. The prior work by Mansfield and Wooldridge [3] and Schwind and Wooldridge [4] considered the effects of pressure with experiments at 5, 10 and 15 atm. The promoting effect of TMSO and HMDSO was observed at all pressures. The authors proposed the increased reactivity observed with the addition of HMDSO and TMSO to syngas mixtures was likely due to effects on the formation and consumption of key radical species, particularly HO_2 and OH, though the exact

pathways were unknown. Two-stage ignition was predicted and observed at higher pressure (15 atm), and the pressure dependence was attributed to the $H+O_2(+M) = HO_2(+M)$ reaction [3]. Perturbation analyses conducted by Mansfield and Wooldridge [3] suggested that disruption of HO_2 formation and increased consumption of HO_2 were likely significant factors contributing to the observed effects. Schwind and Wooldridge [4] computationally considered the direct production of OH radicals from the decomposition of TMSO and concluded the pathway was improbable based on qualitative consideration of TMSO reaction kinetics by analogy with hydrocarbon reaction pathways.

These prior studies indicated OH measurements can provide direct insight into the syngas reaction kinetics effected by TMSO and HMDSO. Thus, the primary objective of the current work was to experimentally measure OH radical time histories during syngas ignition with the addition of varying amounts of HMDSO and TMSO. In the current work, OH data, along with the corresponding observations of pressure time histories and auto-ignition delay times (determined from the pressure time histories during ignition) were analyzed to determine insights on the effects of siloxane addition on syngas combustion kinetics. The interpretation of the results was aided by comparison of the experimental observations of the OH mole fraction and pressure data with chemical kinetics modeling. The experimental approach followed the prior work by Mansfield and Wooldridge [3] and Schwind and Wooldridge [4] where a dilute and fuel-lean syngas composition (1.2% H_2, 2.8% CO, $\phi = 0.1$, by volume) was used as a reference (i.e., baseline) condition and compared with auto-ignition data from mixtures with the addition of 100, 200, and 1000 ppm of TMSO and 100 ppm of HMDSO. A nominally fixed pressure (~5 atm) was used for the experiments to ensure sufficient signal-to-noise for the OH measurements via line-of-sight laser absorption.

Using the results of the experimental measurements, the current predictive understanding of the elementary reaction chemistry of TMSO and HMDSO was also evaluated in the current study. Since the prior work by Mansfield and Wooldridge [3] and Schwind and Wooldridge [4], two important studies of silanes and siloxanes have been completed that are relevant to the current work. Janbazi et al. [17] conducted an experimental study on combustion of tetramethylsilane (TMS), including the creation of a reaction mechanism to describe TMS combustion. As part of the work by Janbazi et al. [177], they included TMSO reaction chemistry. In a separate recent study, Huang and Chen [18] completed molecular dynamics studies of HMDSO decomposition chemistry and reaction kinetics. Their work included developing an elementary reaction mechanism for HMDSO combustion and validating the simulation predictions with results from HMDSO combustion experiments. The reaction mechanisms from the Janbazi et al. [17] and Huang and Chen [18] studies were applied to simulate the ignition studies of the current work, and the results and implications are discussed here.

2. Experimental Methods

2.1. Auto-ignition Delay Time Measurements

A series of auto-ignition experiments for syngas mixtures with TMSO and HMDSO were conducted using the University of Michigan Rapid Compression Facility (UM-RCF) at initial conditions targeting 5 atm and temperatures ranging from 1000 to 1100 K. The UM-RCF is a system uniquely designed to create a homogeneous test volume with uniform high temperature and pressure conditions using an isentropic compression process. The time-resolved pressure data are used to determine the auto-ignition delay times of test gas mixtures at different temperature and pressure conditions. A detailed description of the UM-RCF performance can be found in

Donovan et al. [19]. Briefly, the UM-RCF consists of three main parts: the driver section, the driven section, and the test section. Before initiating experiments, a free-piston (a sabot with a replaceable nose cone) is placed between the driver section and driven section. The driven section is initially evacuated and filled with the test gas mixture. The driver section is subsequently filled with high-pressure air. The two sections are separated by a globe valve and a Mylar sheet. When the globe valve is opened, the sheet ruptures, releasing the pressurized air and propelling the piston through the driven section. This process compresses the test gas mixture into the test section, and at the end of the compression stroke, the piston seals the test section through an interference fit with the test section wall.

All test mixtures were prepared in a stainless-steel mixing tank with an automatic stirring mechanism and were mixed for at least two hours prior to use. The mixture composition was determined by measuring the relative partial pressure of each gas component. The test gas mixture used in this study was composed of 1.2% H_2, 2.8% CO, 21.6% O_2 by volume, with the remaining volume a mixture of N_2 and Ar (adjusted to control test temperatures). The resulting equivalence ratio, ϕ, was 0.1 with air levels of dilution. The fuel-lean condition was used to ensure homogenous ignition in the test section and to facilitate comparison with prior UM-RCF studies. As shown in Mansfield et al. [20], syngas mixtures with higher equivalence ratios can lead to weak ignition with inhomogeneous behavior. Such conditions are not suitable for OH measurements due to the gradients created by local ignition sites. For siloxane experiments, 100, 200, and 1000 ppm of TMSO and 100 ppm of HMDSO were added to the gas mixture. Ultra-high purity O_2, Ar, N_2, and CO, and pre-purified grade H_2 (all sourced from Purity Plus) were used. TMSO and HMDSO with purities of $\geq$ 97.5% and 98.5% respectively were obtained from Sigma Aldrich.

For all experiments, the pressure time history was obtained in the test section using a pressure piezoresistive transducer (Kistler 4045A2) and coupled charge amplifier (Kistler 4618A0) with 100 kHz sampling frequency. Typical uncertainty in the pressure measurements is estimated as $\leq 2\%$ of total range (~ 0.1 atm) and is primarily attributed to noise from the mechanical impact of the piston seating at the end of compression. All data were recorded using a digital data acquisition system (National Instruments cDAQ-9178 chassis coupled with analog input model cDAQ-9223).

A typical pressure time history during a UM RCF auto-ignition experiment is shown in **Fig. 1.** The free piston compresses the test gas mixture into the test volume causing a rapid increase in pressure in the test section until the piston is seated at the end of compression (EOC). The time at the EOC is set as t = 0 s. After EOC, the pressure decreases slightly due to heat transfer to the walls of the RCF (P_{min}) before a second large pressure increase associated with the auto-ignition event is observed. The corresponding temperatures throughout the experiment are calculated using isentropic state relations, the experimentally measured pressure data, and the thermochemical properties of the test-gas mixture. The pressure data are processed using a 75-point smoothing algorithm prior to analysis to reduce noise from the mechanical impact of the piston seating and to reduce electronic noise. The effect of changing the range of the smoothing algorithm by $\pm$ 50% is considered in the uncertainty of the experiments. Each experiment is characterized by an initial thermodynamic state, which is defined as the average pressure and temperature from the EOC to the time of minimum pressure. Data processing was the primary source of uncertainty in the state conditions, yielding typical uncertainties of 1-2% for P and T. For this study, P ranged from 4.68 to 5.27 atm and T ranged from 1010 to 1080 K. The equivalence ratio was fixed at $\phi = 0.1$ for all experiments.

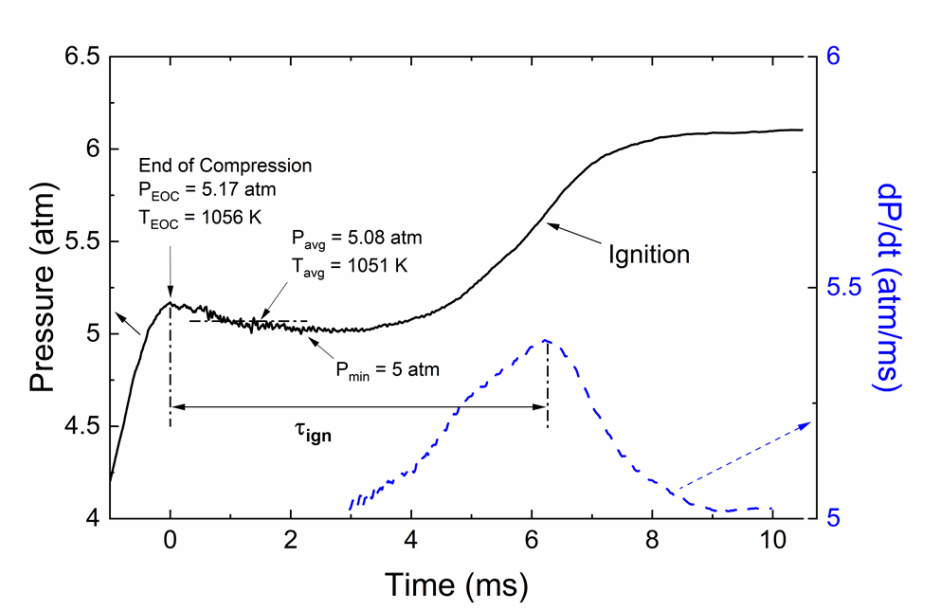

Fig. 1: Typical pressure time history during auto-ignition of 1.2% H_2, 2.8% CO, 20% O_2, 4.5% Ar and 71.5% N_2 (by volume).

As shown in **Fig. 1**, the auto-ignition delay time for each experiment is defined as the time interval from the EOC to the time of maximum rate of pressure rise. The primary source of uncertainty in determining the auto-ignition delay time is due to data processing of the pressure measurements, resulting in a typical uncertainty of less than 3%.

The chemiluminescence emitted during ignition was recorded using a high-speed camera through a transparent polycarbonate end-wall of the test section for each ignition experiment. The imaging was used to confirm homogeneity of the test-gas mixture in the test section, which enables analysis of the laser absorption diagnostic (described in detail below). For the imaging, a high-speed camera (Phantom V711-32G-MAG-C, 512 ×512 pixels, CMOS array, frame rate of 25,000 frames per second, 39.6 μs exposure time), was used with a 50 mm lens (Navitar, F0.95), a 62 mm lens (HOYA +2 Zoom), and a 62 mm UV(0) filter (HOYA). Typical images during ignition are

presented in **Fig. 2**. The time of the images is relative to the end of compression (t = 0 ms). For all experiments, the ignition events were quite homogeneous, as seen in the images. The temperature range of the current work was limited by a combination of the test time, signal-to-noise ratio of the laser absorption signal and the syngas ignition regime.

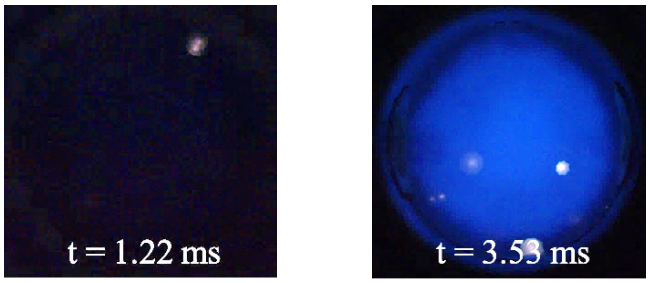

Fig. 2: Typical chemiluminescence imaging (brightness enhanced for clarity) from ignition of syngas with 200 ppm of TMSO (1.2% H_2, 2.8% CO, 200 ppm TMSO, $\phi = 0.1$, P = 5 atm, T = 1050 K). The images correspond to the time of minimum pressure (1.22 ms) and the time of ignition determined from the pressure data (3.53 ms) relative to the end of compression (0 ms).

2.2. OH Laser-Absorption Measurements

Figure 3 is a schematic of the UM-RCF test section, laser absorption diagnostic, and high-speed imaging setup. The laser absorption diagnostic was used to measure OH concentration during ignition. The high-speed imaging camera was used to record chemiluminescence during ignition and thereby assess the homogeneity of the gases in the test section as shown in **Fig. 2**. The ultraviolet (UV) narrow line laser-absorption diagnostic used to measure OH mole-fraction during ignition is described in detail in Mansfield [21]. Briefly, the diagnostic consists of a diode-pumped solid-state laser (Coherent Verdi G7) operating at ~7 W and 532 nm that pumps a continuous-wave ring-dye laser (Coherent 899-05) operating with Rhodamine 6G dye. The ring-dye laser uses

intracavity frequency-doubling to generate a UV beam, which is directed to the UM-RCF test section through a fiber optic cable (Multimode Fiber Optics, Inc., PCU600-10-SF, 10 m length). The OH measurements were made along the line-of-sight orthogonal to the axis of the RCF and 25mm from the end wall of the test section. The laser is tuned to the resonant frequency of the $R_1(5)$ transition of $A^2\Sigma^+ \leftarrow X^2\Pi_i(0,0)$ band of the OH spectrum ($\nu_0 = 32606.556 cm^{-1}$, 306.687 nm,). A wavemeter and power meter are used to monitor the UV emission wavelength and power. The UV laser beam is split into two beams prior to entering the test section for differential absorption measurements. A portion of the laser emission is sent directly to a dual-input differential photodetector sensor system (Thorlab PDB220A2) via a fiberoptic cable, while the other portion of the laser emission is passed through the RCF test section before being focused onto the other electronically-matched photodetector in the sensor. To maintain the proper resonant frequency the wavelength is tuned to the maximum laser absorption across a flame prior to each experiment. The transparent sapphire windows of the test section are heated for ~ 7 mins prior to the start of each experiment using integrated resistance heaters to avoid water condensation during the experiment.

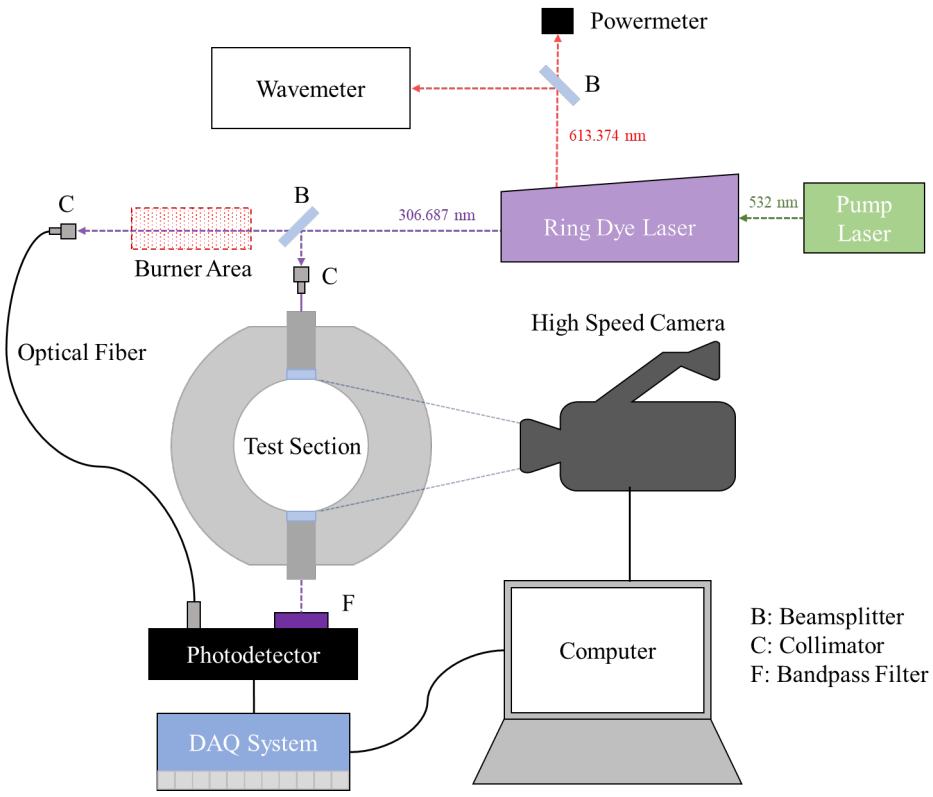

Fig. 3: Schematic of UM-RCF test section and laser-absorption spectroscopy system.

The fractional UV laser absorption is converted to OH mole fraction by applying the Beer-Lambert expression

$$\left(\frac{I}{I_0}\right)_\nu = \exp\left(-\int_0^L k_\nu dx\right) \quad (1)$$

where k_ν is the wavelength-dependent absorption coefficient, I_o is the intensity of incident laser emission, I is the laser emission intensity measured after propagation through the test section, and L is the path length through the absorbing medium. The path length is approximately 3.5 cm (based on chemiluminescence imaging) with a beam diameter of approximately 3 mm focused at the center of the test section. The absorption coefficient, k_ν, can be defined as the product of the line strength (S) and the line-shape function (φ_ν) [22,23] and assuming mixture homogeneity along the path length, the OH mole fraction is determined using the following equation:

$$\chi_{OH} = -\frac{1}{S\varphi_\nu PL}\ln\left(\frac{I}{I_0}\right)_\nu \quad (2)$$

where S is the transition strength of the $R_1(5)$ line, φ_ν is the line-shape function, P is the pressure, and χ_{OH} is the OH mole fraction. The transition strength of the $R_1(5)$ line is a function of temperature and various known spectroscopic parameters. The line-shape function, φ_ν, is a function of temperature, pressure, and the test gas mixture composition. Doppler and collisional broadening were considered in the current work and a Voigt convolution of the two factors was applied to determine the line shape function. Detailed descriptions of calculation methods can be found in Mansfield [21] and Donovan et al. [23]. Collisional broadening by silicon compounds (TMSO and HMDSO) was not considered due to low concentrations of these species in the test gas mixtures. As discussed in Donovan et al. [23], uncertainty in the OH mole-fraction calculation is the result of the prescribed uncertainty in the path length, the thermodynamic state, and the data processing. The uncertainty in the OH mole-fraction calculations for this study was +30/-13%.

Typical OH data are presented in **Fig. 4**. Details on the analysis of the laser emission data are provided in the Supplemental Material. For all experiments, there was negligible absorption of the laser emission before the end of compression, and peak absorption consistently occurred at the time of ignition based on the pressure time history. Laser data near the end of compression were excluded from the OH analysis due to the large mechanical noise caused by the impact of the free piston. Auto-ignition delay times determined from the OH data (defined as the time from EOC to the time of maximum OH) were virtually identical to τ_{ign} determined exclusively from the P data.

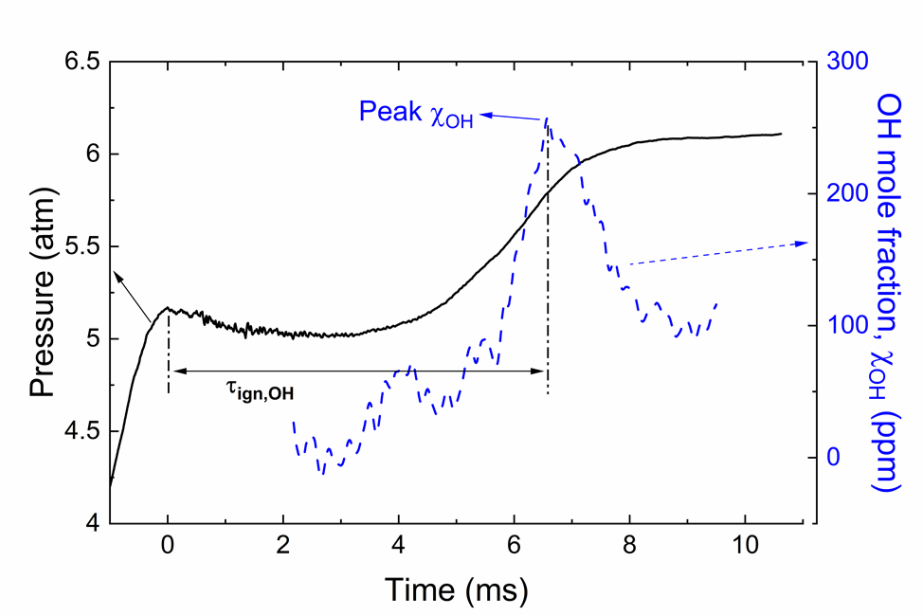

Fig. 4: Typical experimental results for χ_{OH} (blue dash line) and pressure (black solid line) for a reference syngas mixture (1.2% H_2, 2.8% CO, 20% O_2, 4.5% Ar, 71.5% N_2 by volume) at P = 5.08 atm and T = 1051 K.

2.3 Kinetics Modeling

In the current work, the experimental observations for the OH and pressure time-histories and the autoignition delay times are compared with results of detailed kinetics modeling of syngas ignition using the reaction mechanism for syngas created by Li et al. [24]. For TMSO, the TMS reaction mechanism by Janbazi et al. [17] was used, which includes the syngas reaction chemistry from Li et al. [24] and TMSO reaction chemistry. For HMDSO, the reaction mechanism created by Huang and Chen [18] was initially tested, but there was poor agreement with the syngas baseline results for ignition delay time (with model predictions 8 to 10 times faster than the experimental measurements). Thus, a new reaction mechanism was created by combining the HMDSO reaction chemistry from Huang and Chen [18] with the syngas mechanism by Li et al. [24]. The HMDSO reaction mechanism and associated thermodynamic data are provided in the Supplemental Material.

Recent work by Chatelain et al. [25,26] compared six reaction mechanisms for silane (SiH_4) including prior work from the UM-RCF research group (Miller et al. [27]) and includes more recent estimates for some Si/H/O reactions. Although silanes and siloxanes share some similar molecular structures, their detailed reaction pathways are quite different. Comparison of the reaction chemistry indicates silane reaction pathways are not active in TMSO and HMDSO ignition systems. However, for completeness, silane chemistry from Chatelain et al. [255,266] was incorporated into the TMSO and HMDSO mechanisms used in the current study. The simulations showed no observable differences compared with the original mechanisms, and thus the original reaction mechanisms without silane reaction chemistry were used throughout this study.

For all model simulations, the 0-D Closed Homogeneous Batch Reactor/Chemkin program (version 10131, x64) [28] was used. He et al. [22] provide detailed discussion on various modeling approaches applicable to UM-RCF experiments, including a comparative analysis of the different approaches. Consistent with the recommendations by He et al. [22], the experimental conditions (average T and P, and reactant mixture) were used here as the initial conditions for the simulations, and ignition was modeled as a constant internal energy and constant volume system.

3. Results

3.1 Auto-Ignition Delay Time

The auto-ignition experiments were conducted in the UM-RCF for syngas mixtures with 100, 200, and 1000 ppm of TMSO and 100 ppm of HMDSO at conditions of ~5 atm, 1010-1080 K, and $\phi = 0.1$. A summary of the experimental conditions and results for auto-ignition delay time and the key OH features are provided in the Supplemental Material. The auto-ignition delay time results for the syngas mixtures with TMSO and HMDSO are presented in the Arrhenius diagram

in **Fig. 5**. The results show typical linear log τ_{ign} versus 1/T behavior for each mixture composition, and it is evident the addition of both TMSO and HMDSO to the syngas mixtures systematically enhanced reactivity yielding faster (i.e., smaller) auto-ignition delay times. Specifically, compared with the syngas mixtures without siloxanes, the addition of 100 ppm TMSO reduced the ignition delay time by up to 35%, and 100 ppm HMDSO decreased the ignition delay time by 53% at similar experimental conditions. The 1000 ppm TMSO mixtures yielded auto-ignition delay times more than a factor of three faster than the baseline syngas mixture. Best fit linear regressions for τ_{ign} for each mixture are provided in **Fig. 5** and **Table 1**. The activation energies are consistent for the different mixtures, except for 200 ppm TMSO, which has the smallest temperature range for fitting. The auto-ignition delay time data are in excellent agreement with findings from Schwind and Wooldridge [4] and Mansfield and Wooldridge [3] for syngas with trace TMSO at similar pressure and temperatures. Comparison of the ignition data from the current work and the previous RCF studies is provided in the Supplemental Material.

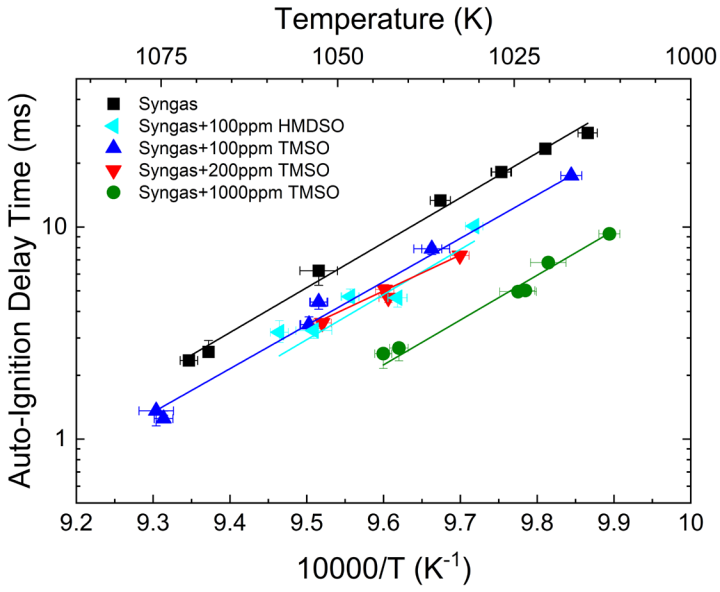

Fig. 5: Comparison of auto-ignition delay time data of syngas mixtures (1.2% H_2, 2.8% CO, and φ = 0.1) with the addition of TMSO or HMDSO (average pressure of 5.05 atm for all experiments presented in the figure). The error bars are the uncertainty in the measurements. Some uncertainties are smaller than the size of the symbols. The lines are linear regressions for each mixture in the form $\tau_{ign}\ [ms] = A\ \exp(E_a/RT)$. Fit parameters for the regressions are provided in **Table 1**.

Table 1: Best-fit results for the pre-exponential factor A, activation energy E_a, and corresponding standard errors (SE) and coefficient of determination (R^2) of the linear regression fits for the auto-ignition delay time ($\tau_{ign}\ [ms] = A\ \exp(E_a/RT)$) results presented in **Fig. 5**.

Mixture	A [ms]	SE_A[ms]	E_a [kcal/mol]	SE_{Ea} [kcal/mol]	R^2
Syngas	6.9×10^{-20}	1.0×10^{-19}	95.9	3.1	0.995
Syngas + 100 ppm HMDSO	1.0×10^{-18}	8.0×10^{-17}	89.2	16.6	0.906
Syngas + 100 ppm TMSO	3.8×10^{-19}	8.3×10^{-19}	91.3	4.5	0.991
Syngas + 200 ppm TMSO	4.7×10^{-17}	2.0×10^{-16}	81.1	8.8	0.977
Syngas + 1000 ppm TMSO	1.7×10^{-18}	5.8×10^{-18}	86.5	6.8	0.976

3.2 OH Time Histories

Figure 6 presents typical OH mole fraction and the corresponding pressure time histories from syngas, TMSO, and HMDSO experiments with nominally the same temperature (1042 to 1052 K). The general shape of the OH time histories were consistent regardless of the presence of TMSO or HMDSO, with rapid formation of OH followed by rapid consumption. For all experiments, the time of maximum OH was coincident with the ignition delay time determined

from the pressure data. However, for all experiments with siloxanes, OH was formed earlier than for the baseline syngas mixtures, as seen in the data in **Fig. 6**. The maximum values of OH mole fraction were similar for the baseline syngas, 100 ppm and 200 ppm TMSO, and the 100 ppm HMDSO mixtures as seen in **Fig. 7**; however, the maximum level of OH was significantly higher for the 1000 ppm TMSO mixtures.

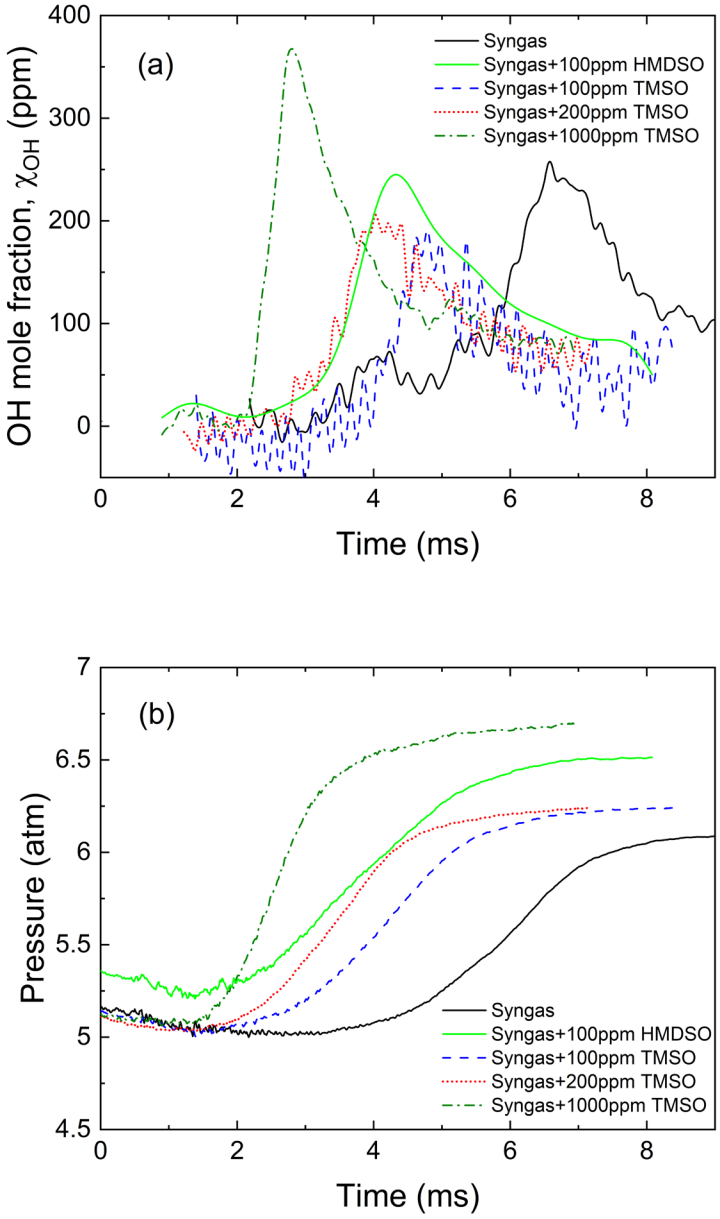

Fig. 6: Comparison of (a) OH mole-fraction and (b) corresponding pressure time histories for the ignition of syngas mixtures (1.2% H_2, 2.8% CO, ϕ = 0.1) with addition of TMSO and HMDSO. The average temperatures and pressures are 1051 K and 5.08 atm for pure syngas, 1051 K and 5.08 atm for 100 ppm TMSO, 1050 K and 5.11 atm for 200 ppm TMSO, 1042 K and 5.10 atm for 1000 ppm TMSO, and 1052 K and 5.36 atm for 100 ppm HMDSO.

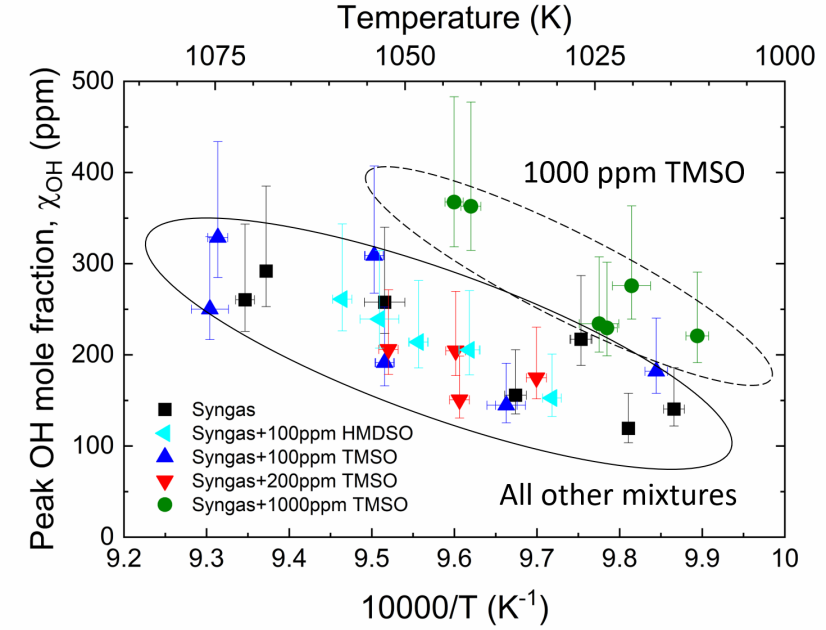

Fig. 7: Maximum OH mole fraction (χ_{OH}) during ignition of syngas mixtures (1.2% H_2 and 2.8% CO) with TMSO or HMDSO at an average pressure of 5.05 atm and ϕ = 0.1.

As seen in **Fig. 6**, the OH data also indicate OH was not completely consumed during the observation period after ignition. The final conditions of ignition experiments are generally defined by thermal equilibrium (e.g., enthalpies of formation and assumptions of complete combustion [22]), and not reaction kinetics; whereas, the formation and removal of OH, rate of heat release rate and pressure rise are determined by the finite rate reaction chemistry. Regarding thermal

equilibrium after ignition, combustion of siloxanes will release significant energy via the formation of solid-phase silica ($SiO_{2,s}$) because the particle nucleation process is highly exothermic. The experimental results indicate progressively higher post-ignition pressure with increasing Si in the mixture (see **Fig. 6**), consistent with heat release from particle formation.

In **Fig. 8**, the OH mole-fraction time histories for the TMSO syngas mixtures have been shifted (e.g., translated) to directly compare the rate of OH formation and consumption rates near the time of ignition. The measurements indicate lower concentrations of TMSO (100 ppm and 200 ppm) do not significantly influence the rate of OH formation or consumption. Thus, the TMSO and HMDSO reactions are not rate limiting to the formation of OH, and TMSO and HMDSO are not directly producing OH. However, at 1000 ppm TMSO, the formation and consumption of OH occur more rapidly compared with the lower TMSO concentrations. This indicates additional OH production reactions are promoted with the higher levels of TMSO, also leading to a higher peak of OH mole fraction as seen in **Fig. 6**. Kinetics modeling provides additional insight into the potential reaction pathways effected by the siloxanes

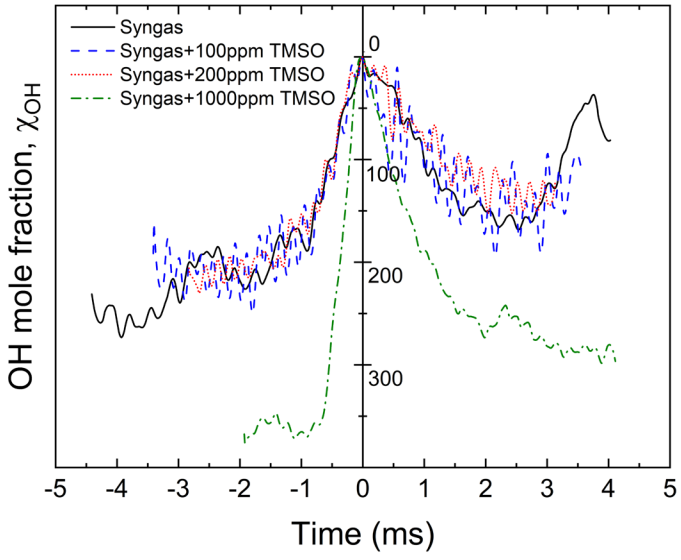

Fig. 8: Comparison of OH time histories where the data have been shifted (i.e., translated) to set the maximum OH value as $\chi_{OH} = 0$ and the time of OH maximum as t = 0 ms, for baseline syngas mixtures (1.2% H_2, 2.8% CO, $\varphi = 0.1$) and syngas mixtures with of TMSO or HMDSO. The temperature of the experiments ranged from 1042 K (1000 ppm TMSO) to 1052 K (100 ppm HMDSO) with an average pressure of 5.12 atm.

4. Discussion

The results of the current work directly confirm OH production is enhanced with the addition of TMSO and HMDSO to syngas mixtures; specifically, OH formation occurs much earlier with the addition of TMSO and HMDSO compared with a baseline syngas mixture. The observation that the OH time histories are shifted in time (see **Fig. 6**), rather than the OH proportionally increasing relative to the amount of TMSO in the mixture (see **Figs. 6-8**) indicates OH is not directly formed by scission of the OH moiety from the TMSO or by reactions directly producing OH from reaction with HMDSO or TMSO. The trends suggest OH is created via reactions where the siloxane kinetics are not rate limiting. The potential reaction pathways affected by the addition of TMSO and HMDSO to syngas are considered here using elementary reaction kinetics modeling for the different reactant mixtures.

4.1. Syngas Reaction Modeling

The baseline syngas reaction kinetics of Li et al. [24] were verified using the experimental data from the current work. Comparison of the model predictions for OH mole fraction and auto-ignition delay time for the reference syngas mixtures (with no organic-silicon compounds in the mixtures) were in good agreement with the experimental measurements (i.e., within the

computational and experimental uncertainties). Model and experimental comparisons, species time histories, sensitivity analysis, and rate of production analysis for the baseline syngas mixture are provided in the Supplemental Material. The results show the OH and auto-ignition delay time data are most sensitive to competition between the $H + O_2 = OH + O$ and the $H+O_2(+M) = HO_2(+M)$ reactions. It is important to note the results and analysis presented here are for the conditions studied and scientific considerations should be used before extrapolating the results or conclusions to other conditions.

4.2. TMSO Reaction Modeling

As described earlier, the TMS reaction mechanism by Janbazi et al. [17] includes TMSO chemistry and incorporates the syngas reaction mechanism by Li et al. [24]. Simulation results using the Janbazi reaction mechanism and experimental results for OH mole-fractions for ignition of syngas and a syngas mixture with TMSO at T = 1050 K are presented in **Fig. 9**. The syngas-only experimental and simulation results are in excellent agreement. For the TMSO mixture, the comparison with the experimental data shows there is a good correlation regarding the shape of the OH time history and the maximum OH mole fraction; however, the effect of the TMSO on the ignition timing is opposite to the experimental observation. The simulation predicts longer ignition delay times with the addition of TMSO to syngas in contrast to the experimental observations.

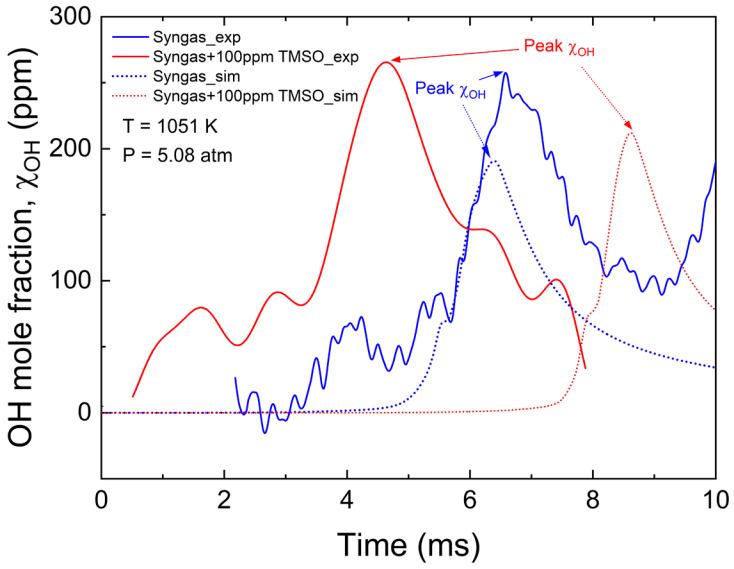

Fig. 9: Comparison of experimental (solid) and simulation (dashed) results for OH mole-fraction using the TMSO reaction mechanism for 1051 K and 5.08 atm. Blue lines are results for syngas ignition and red lines are results for syngas with 100 ppm TMSO.

Comparisons of the auto-ignition delay times and the maximum OH mole fractions for the 100 ppm and 1000 ppm TMSO mixtures are provided in **Figs. 10** and **11**. The Janbazi reaction chemistry predicts a lower activation energy for the TMSO mixtures compared with the experimental data and longer ignition delay times than the experimental measurements for both the 100 ppm and the 1000 ppm TMSO mixtures, with significant discrepancy from the experimental measurements for the 1000 ppm TMSO mixtures. However, the peak OH values predicted by the TMSO mechanism are generally within the scatter of the experimental data and confirm the experimental observation of negligible sensitivity of maximum OH with the addition of 100 ppm TMSO, but significant impact with the addition of 1000 ppm TMSO.

There are several potential sources of discrepancy in the TMSO model, including the thermodynamic data (particularly for radical intermediate silicon containing species), incorrect

rate coefficients (in particular because the TMS and TMSO chemistry was created for low-pressure combustion) or missing reactions. Regarding this last issue, the absence of reactions involving HO_2 with TMSO chemistry may be a problem. Given the critical role of HO_2 in syngas ignition kinetics, the omission could be significant. In addition, the lack of Si-C bond scission reactions, which are present in the HMDSO mechanism, may also be a limitation of the TMSO reaction mechanism. The Si-C scission reactions may contribute to CH_3 radical formation, enhancing OH production and promoting faster ignition. Improving the TMSO reaction chemistry is the subject of on-going fundamental research.

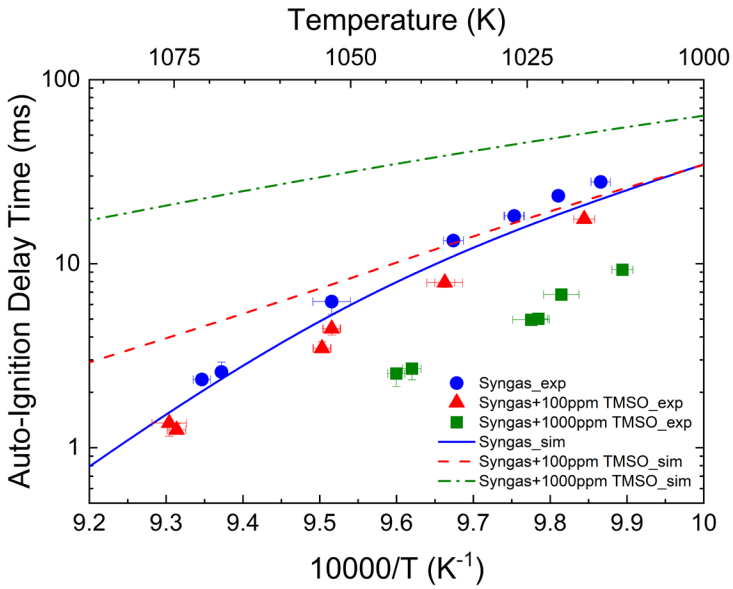

Fig. 10: Comparison between model predictions using the reaction mechanism by Janbazi et al. [17] (lines) and experimental measurements (symbols) of auto-ignition delay times for TMSO and baseline syngas mixtures. Data include pressures from 4.68 to 5.27 atm.

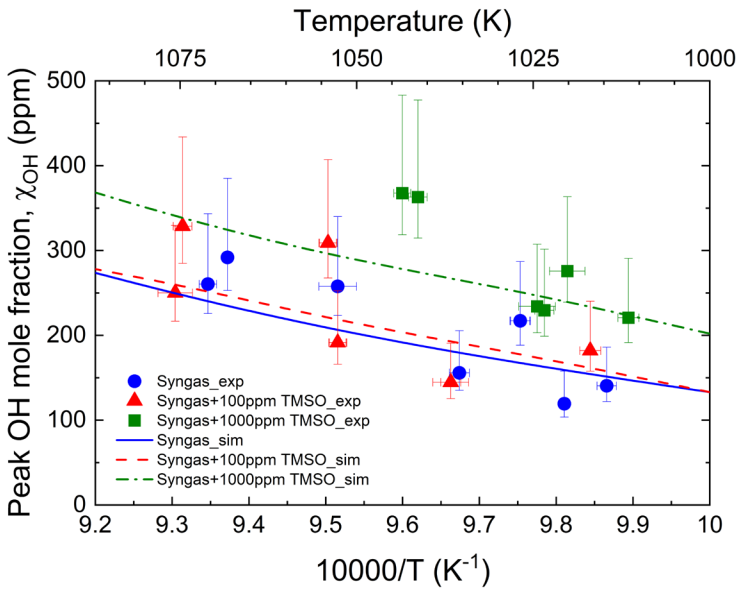

Fig. 11: Comparison between model predictions using the reaction mechanism by Janbazi et al. [17] (lines) and experimental measurements (symbols) of maximum OH for TMSO and baseline syngas mixtures. Data include pressures from 4.68 to 5.27 atm.

The TMSO reaction chemistry was interrogated using sensitivity and rate of production analyses to understand the effect of TMSO on the reaction pathways. The detailed results are provided in the Supplemental Material. Briefly, the analyses indicate the same reactions are important as with the baseline syngas reaction mechanisms, with slight shifts in magnitude. No reactions involving Si-containing species appear in the sensitivity or rate of production analysis for OH with the reaction mechanism by Janbazi et al. [17].

4.3. HMDSO Reaction Modeling

Figure 12 compares model predictions using the HMDSO reaction mechanism with experimental measurements of OH time histories for 1052 K. The model results correctly reproduce the promoting effect of HMDSO on OH formation, consistent with faster ignition delay

time, and the general features of the OH time histories are consistent between the model and the experiments. Specifically, both show the addition of HMDSO leads to earlier production of OH and similar maximum OH (within ~15%).

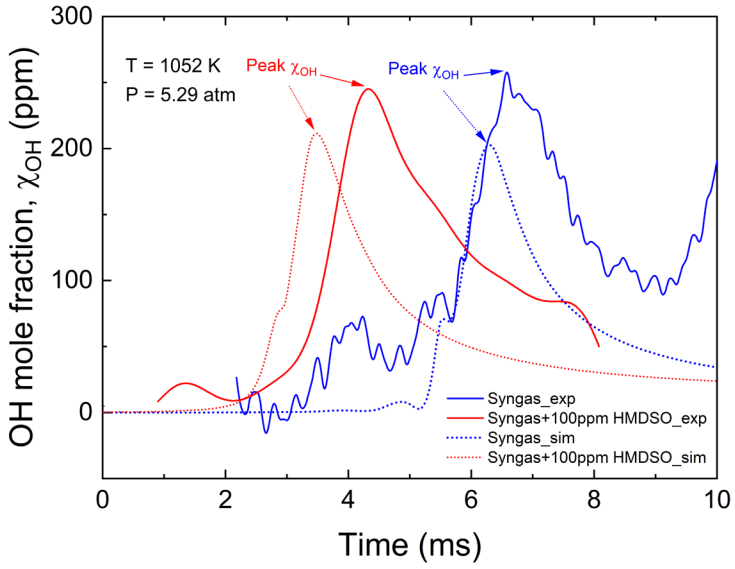

Fig. 12. Comparison of experimental (solid) and simulation (dashed) results for OH mole-fraction using the HMDSO reaction mechanism for 1052 K and 5.29 atm. Blue lines are results for syngas ignition and red lines are results for syngas with 100 ppm HMDSO.

Figures 13 and **14** present the experimental and modeling results for auto-ignition delay time and maximum OH mole fractions for the HMDSO mixtures. While the model predictions for the mixtures with HMDSO are systematically faster than the experimental observations, the ignition delay times are within a factor of two, which is good agreement given the uncertainties in the HMDSO chemistry. The model predictions for the maximum OH values are also in good agreement with the experimental measurements (within the scatter of the experimental data).

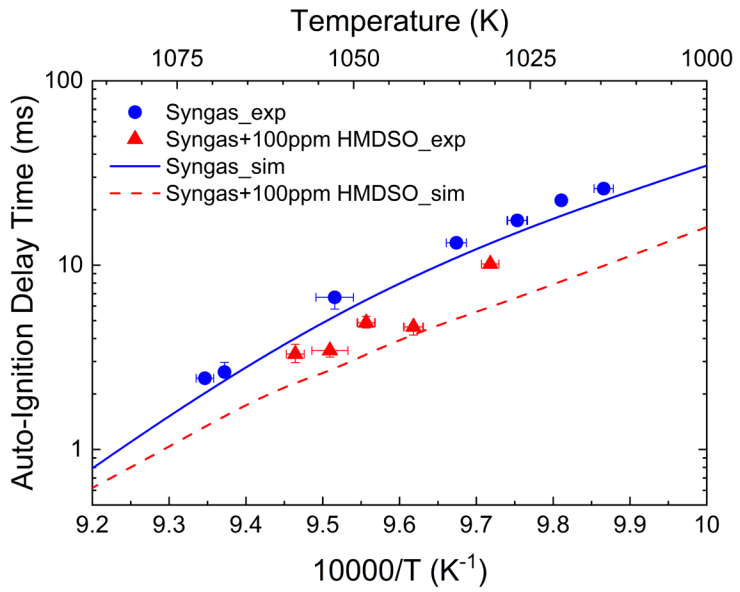

Fig. 13: Comparison between model predictions (lines) and experimental measurements (symbols) of auto-ignition delay times for 100 ppm HMDSO and baseline syngas mixtures. Data include pressures from 4.68 to 5.29 atm.

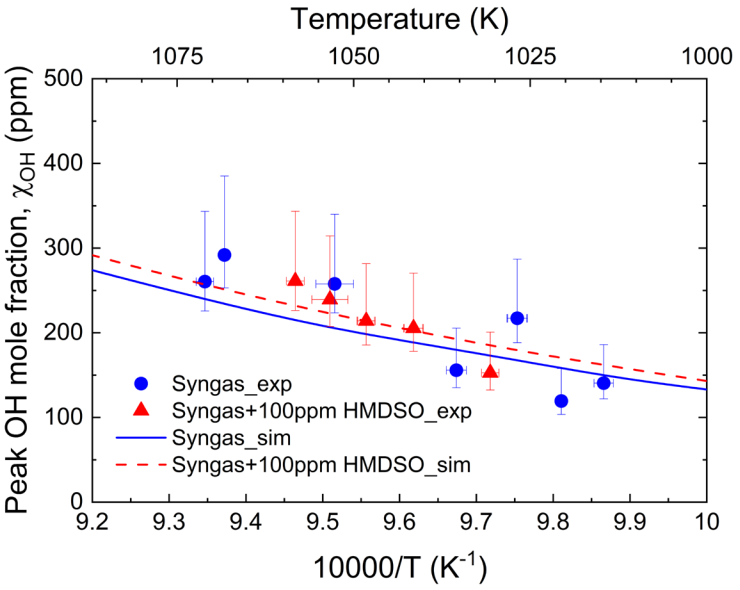

Fig. 14: Comparison between model predictions (lines) and experimental measurements (symbols) of maximum OH for 100 ppm HMDSO and baseline syngas mixtures. Data include pressures from 4.68 to 5.29 atm.

To understand the pathway for HMDSO to accelerate auto-ignition delay times and the time of formation of OH, sensitivity and rate of production analyses were conducted. The results are briefly summarized here, and the details are provided in **Fig. 15**. The HMDSO simulations indicate HMDSO is consumed very rapidly, within 1 ms, correlating with the rapid initial production of HO_2. The $H+O_2$ reactions (forming OH + O and HO_2) were identified as the dominant reactions affecting OH radical formation and consumption during ignition, as found with syngas ignition without siloxanes. However, Si-C scission reaction was also identified as important, indicating HMDSO thermal decomposition chemistry plays a significant role in the very early reaction processes. While methyl radicals will increase the reactivity of the mixture, the sensitivity analysis indicates the mechanism for accelerating ignition and earlier formation of OH is through increased production of H atoms.

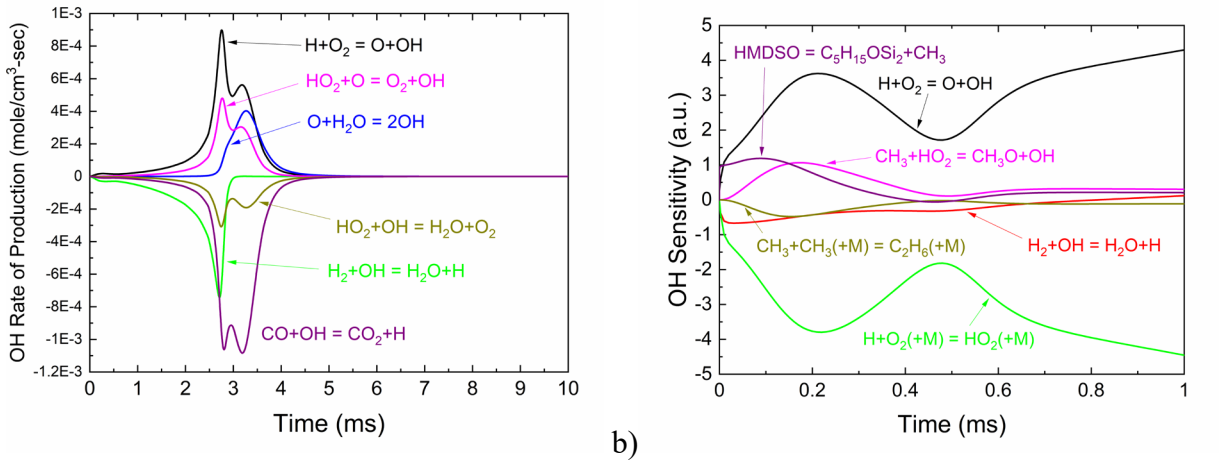

a) b)

Fig. 15: Results for a) rate of production analysis and b) sensitivity analysis for OH for during ignition of HMDSO and syngas (1.2% H_2, 2.8% CO, 100 ppm HMDSO, $\phi = 0.1$, 5 atm, and 1050 K) using the HMDSO chemistry of Huang and Chen [18] and syngas chemistry of Li et al. [24].

5. Conclusions

The effects of TMSO and HMDSO addition on OH during auto-ignition of H_2 and CO mixtures were investigated and quantified in the current work. The results show earlier formation of OH with the addition of TMSO and HMDSO to syngas mixtures at 5 atm in the temperature range of 1010-1080 K. For mixtures with siloxane mole fractions of 100 ppm and 200 ppm, similar maximum values of OH mole fractions were measured. However, for 1000 ppm TMSO, increased OH production and consumption were observed, indicating a shift in the dominant reaction kinetics. The OH results for the mixtures with lower levels of siloxane addition show TMSO is not a direct source of OH. In addition, because the OH values did not increase with increasing TMSO content in the reactant mixture, the experimental results indicate TMSO is not a rate-limiting source of OH radicals. Comparison of the OH data for TMSO and HMDSO indicate the reaction pathway causing the earlier formation of OH may be similar for the two compounds, specifically, rapid decomposition leads to increased production of H atoms, which then accelerates the production of OH via $H + O_2 = OH + O$.

Comparison of the experimental data with modeling using elementary reaction mechanisms for TMSO and HMDSO showed good agreement (within a factor of two for auto-ignition delay time and within the scatter for maximum OH) for HMDSO, but considerable discrepancies for TMSO (where the reaction mechanism indicated a decelerating effect with TMSO addition). The reaction mechanisms will need considerable additional validation and verification beyond the current work, but provide a framework to guide further fundamental kinetics experiments, and the OH results provide important quantitative data to test and further develop siloxane reaction kinetics.

Acknowledgements

This work was performed under the auspices of the Office of Basic Energy Sciences, Division of Chemical Sciences, Geosciences, and Biosciences, U.S. Department of Energy (DOE). The work at the University of Michigan was supported under award number DE-SC0019184. The work at Argonne was supported under contract number DE-AC02-2006CH11357 and FWP 29855 "Fundamental Chemical Kinetics of Siloxane and Silicon Compounds".

Declaration of competing interest

The authors declare that they have no known competing financial interests or personal relationships that could have appeared to influence the work reported in this paper

References

1. M. Bachmann, S. Völker, J. Kleinekorte, A. Bardow, Syngas from what? Comparative life-cycle assessment for syngas production from biomass, CO2, and steel mill off-gases, ACS Sustainable Chemistry & Engineering 11 (2023) 5356–5366.
2. J.J. Bolívar Caballero, I.N. Zaini, W. Yang, Reforming processes for syngas production: A mini-review on the current status, challenges, and prospects for biomass conversion to fuels, Appl. Energy Combust. Sci. 10 (2022).
3. A.B. Mansfield, M.S. Wooldridge, The effect of impurities on syngas combustion, Combust. Flame 162 (2015) 2286–2295.
4. R.A. Schwind, M.S. Wooldridge, Effects of organic silicon compounds on syngas auto-ignition behavior, Combust. Flame 212 (2020) 234–241.
5. M. Chaos, F.L. Dryer, Syngas combustion kinetics and application, Combust. Sci. Technol. 180 (2008) 1053–1096.
6. O. Mathieu, J. Hargis, A. Camou, C. Mulvihill, E.L. Petersen, Ignition delay time measurements behind reflected shock-waves for a representative coal-derived syngas with and without NH_3 and H_2S impurities, Proc. Combust. Inst. 35 (2015) 3143–3150.
7. O. Mathieu, M.M. Kopp, E.L. Petersen, Shock-tube study of the ignition of multi-component syngas mixtures with and without ammonia impurities, Proc. Combust. Inst. 34 (2013) 3211–3218.
8. O. Mathieu, J.W. Hargis, E.L. Petersen, J. Bugler, H.J. Curran, F. Güthe, The effect of impurities on ignition delay times and laminar flame speeds of syngas mixtures at gas turbine conditions, ASME Turbo Expo 2014: Turbine Technical Conference and Exposition, Düsseldorf, Germany, June 16–20, 2014, Vol. 4A: Combustion, Fuels and Emissions.

9. P. Glarborg, Hidden interactions – Trace species governing combustion and emission, Proc. Combust. Inst. 31 (2007) 77–98.
10. S. Rasi, J. Lehtinen, J. Rintala, Determination of organic silicon compounds in biogas from wastewater treatments plants, landfills, and co-digestion plants, Renew. Energy 35 (2010) 2666–2673.
11. S.M. Suh, M. Zachariah, S. Girshick, Modeling particle formation during low-pressure silane oxidation: detailed chemical kinetics and aerosol dynamics, J. Vac. Sci. Technol. A 19 (2001) 940–951.
12. B. Tansel, S.C. Surita, Oxidation of siloxanes during biogas combustion and nanotoxicity of Si-based particles released to the atmosphere, Environ. Toxicol. Pharmacol. 37 (2014) 166–173.
13. Q. Meng, Fundamental studies of organic silicon combustion chemistry and characterizing the presence of silicon species in landfill and sludge gas, Ph.D. Thesis, University of Michigan, Ann Arbor, 2023.
14. H.K. Chagger, D. Hainsworth, P.M. Patterson, M. Pourkashanian, A. Williams, The formation of SiO2 from hexamethyldisiloxane combustion in counterflow methane-air flames, Proc. Combust. Inst. 26 (1996) 1859–1865.
15. O.M. Feroughi, L. Deng, S. Kluge, T. Dreier, H. Wiggers, I. Wlokas, C. Schulz, Experimental and numerical study of an HMDSO-seeded premixed laminar low-pressure flame for SiO2 nanoparticle synthesis, Proc. Combust. Inst. 36 (2017) 1045–1053.
16. R.S. Chrystie, H. Janbazi, T. Dreier, H. Wiggers, I. Wlokas, C. Schulz, Comparative study of flame-based SiO2 nanoparticle synthesis from TMS and HMDSO: SiO-LIF concentration measurement and detailed simulation, Proc. Combust. Inst. 37 (2019) 1221–1229.

17. H. Janbazi, Y. Karakaya, T. Kasper, C. Schulz, I. Wlokas, S. Peukert, Development and evaluation of a chemical kinetics reaction mechanism for tetramethylsilane-doped flames, Chem. Eng. Sci. 209 (2019) 115209.
18. Y. Huang, H. Chen, A detailed reaction mechanism for hexamethyldisiloxane combustion via experiments and ReaxFF molecular dynamics simulations, Int. J. Chem. Kinet. 56 (2024) 131–149.
19. M.T. Donovan, X. He, B.T. Zigler, T.R. Palmer, M.S. Wooldridge, A. Atreya, Demonstration of a free-piston rapid compression facility for the study of high-temperature combustion phenomena, Combust. Flame 137 (2004) 351–365.
20. A.B. Mansfield, M.S. Wooldridge, High-pressure low-temperature ignition behavior of syngas mixtures, Combust. Flame 161, 2014, 2242–2251.
21. A.B. Mansfield, Experimental study of synthesis gas combustion chemistry and ignition behaviors, Ph.D. Thesis, University of Michigan, 2014.
22. X. He, B.T. Zigler, S.M. Walton, M.S. Wooldridge, A. Atreya, A rapid compression facility study of OH time histories during iso-octane ignition, Combust. Flame 145 (2006) 552–570.
23. M.T. Donovan, Experimental study of the role of OH in SiO_2 particle nucleation in SiH_4 combustion using UV absorption spectroscopy, Ph.D. Thesis, University of Michigan, 2003.
24. J. Li, Z. Zhao, A. Kazakov, M. Chaos, F.L. Dryer, J.J. Scire Jr., A comprehensive kinetic mechanism for CO, CH_2O, and CH_3OH combustion, Int. J. Chem. Kinet. 39 (2007) 109–136.
25. K.P. Chatelain, Y. He, R. Alharbi, R. Mével, E.L. Petersen, D.A. Lacoste, Current status of the high-temperature kinetic models of silane: Part I. Pyrolysis, Combust. Flame 227 (2021) 526-537.

26. K.P. Chatelain, Y. He, S. Javoy, R. Mével, E.L. Petersen, D.A. Lacoste, Current status of the high-temperature kinetic models of silane: Part II. Oxidation, Combust. Flame 227 (2021) 538-549.

27. T.A. Miller, M.S. Wooldridge, J.W. Bozzelli, Computational Modeling of the $SiH_3 + O_2$ Reaction and Silane Combustion" Combust. Flame, 137 (2004) 73-92.

28. CHEMKIN, release 10131 (x64), Reaction Design: San Diego, 2011.